

## Artificially Induced Perturbations in Chirped Magneto-Optical Bragg Gratings

Fredrik Jonsson<sup>1\*</sup> and Christos Flytzanis<sup>2</sup>

<sup>1</sup>*National Microelectronics Research Centre, Lee Maltings, Prospect Row, Cork, Ireland*

<sup>2</sup>*Laboratoire Pierre Aigrain, Ecole Normale Supérieure, F-75231 Paris, France*

\*Corresponding author. Email: fredrik.jonsson@nmrc.ie

### Abstract

We report on theoretical analysis of magneto-optically induced longitudinal perturbations in chirped magneto-optical Bragg gratings. The induced perturbations considered are of Lorentzian shape, with a spatial extent considerably larger than the spatial grating period but at least an order of magnitude less than the geometrical length of the grating. In the numerical simulation of the proposed device, we show on a high polarization state selectivity in the region of the perturbation, with resonance peaks of transmission for circularly polarized orthogonal components possessing a full width at half maximum as narrow as 0.18 nm, meanwhile being separated by 0.6 nm.

### Introduction

Currently one major research direction in photonics is towards bringing photonic devices into a true nano-technological scale, with optical routing and switching ultimately performed in a sub-micrometer length scale. However, in today's high-performance optical systems the necessary interaction lengths are still rather in the millimetre order, with typical devices of fiber Bragg gratings and waveguiding structures in silica. In this respect, for these macroscopic systems, the introduction of magneto-optically induced local perturbations along the light path imposes the interesting feature that the lifting of the polarization state degeneracy can be locally exploited in the spectrum, leaving other essential requirements such as a fixed spectral window width and position unchanged. It is the purpose of this work to show on the possibility of a high polarization state selectivity in weakly modulated gratings by introducing a magneto-optically induced perturbation of a macroscopic spatial extent.

In this paper, we focus on chirped optical gratings possessing a linear magneto-optical effect. In the absence of a magnetic field, this class of gratings provide a flat window of reflection, with its boundaries determined by the extreme values taken by the spatially varying grating period. Furthermore, we consider magneto-optically induced perturbations of Lorentzian shape, with a spatial extent which is considerably larger than the spatial grating period but at least an order of magnitude less than the geometrical length of the grating. In a linear magneto-optical medium as here considered, the complex-valued envelope of the electric polarization density obeys the local constitutive relation [1]

$$\mathbf{P}_\omega = \varepsilon_0[(n^2(z) - 1)\mathbf{E}_\omega + i\mathbf{E}_\omega \times \mathbf{g}(z)],$$

in which  $n(z)$  is the refractive index and  $\mathbf{g}(z)$  the magneto-optically induced gyration vector. The refractive index distribution  $n(z)$  is in the present case modulated around a bias index  $n_0$  with a bias spatial grating period of  $\Lambda$ , as

$$[n^2(z) - n_0^2]/n_0 = a_c f(z) \cos [(2\pi/\xi) \ln(1 + \xi z/\Lambda)],$$

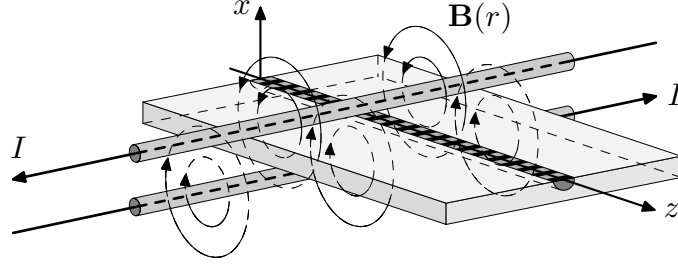


Figure 1: Schematic illustration of a possible setup for magneto-optical generation of perturbations in a grating inscribed in an optical waveguide along the  $z$ -axis.

where  $a_c$  is the peak modulation strength of the grating,  $f(z)$  an apodization function being unity in the active region and smoothly approaching zero at the ends of the grating, and  $\xi$  the chirp parameter describing the strictly increasing or decreasing deviation of the local grating period from the bias.

For the present case, we assume a gyration vector collinear with the direction of wave propagation, taken as the  $z$ -axis of the geometry, and that its spatial distribution takes the form of a Lorentzian perturbation,

$$\mathbf{g}(z) = g(z)\mathbf{e}_z = \frac{g_p}{1 + 4(z - z_p)^2/w_p^2}\mathbf{e}_z,$$

where  $g_p$  is the peak value of the perturbation,  $z_p$  its spatial position, and  $w_p$  its half-maximum width. To fix the ideas as outlined in this paper, this shape of the perturbation is what would result, for example, from an induction in the presence of a wire carrying an electric current across and in the vicinity of a spatially modulated magneto-optical waveguide, as schematically illustrated in Fig. 1. However, it should be emphasized that the exact implementation of the setup for applying the magnetic field is not fixed by this schematic, neither are the features of the introduction of magneto-optically induced perturbations limited to the Lorentzian distribution.

In this model of the grating, the local resonance vacuum wavelength  $\lambda_{\text{loc}}^\pm$  as function of the spatial coordinate  $z$  follows from classical Bragg theory as twice the effective optical period of the grating, as experienced by the respective left and right circularly polarized components of the light, or

$$\lambda_{\text{loc}}^\pm(z) = 2n_0(\Lambda + \xi z)(1 \mp g(z)/2n_0^2).$$

In order to separate equations of evolution for circularly polarized envelopes of forward and backward travelling components, the optical wave is in a circularly polarized basis  $\mathbf{e}_\pm = 2^{-1/2}(\mathbf{e}_x \pm i\mathbf{e}_y)$  taken as

$$\mathbf{E}_\omega = [\mathbf{e}_+ A_+^f(z) + \mathbf{e}_- A_-^f(z)] \exp(i\omega n_0 z/c) + [\mathbf{e}_+^* A_+^b(z) + \mathbf{e}_-^* A_-^b(z)] \exp(-i\omega n_0 z/c),$$

where ‘ $\pm$ ’ in the subscripts denotes left/right circular polarization state. By assuming slowly varying apodization and an adiabatically changing grating period, subsequently applying the slowly varying envelope approximation [2], the wave equation is cast into coupled mode

equations for the field envelopes as

$$\frac{\partial A_{\pm}^f(z)}{\partial z} - i\kappa f(z) \exp \left[ i\frac{2\pi}{\xi} \ln \left( 1 + \frac{\xi z}{\Lambda} \right) - i\frac{2\omega n_0}{c} \left( 1 \mp \frac{g(z)}{2n_0^2} \right) z \right] A_{\mp}^b(z) = 0, \quad (1a)$$

$$\frac{\partial A_{\mp}^b(z)}{\partial z} + i\kappa f(z) \exp \left[ -i\frac{2\pi}{\xi} \ln \left( 1 + \frac{\xi z}{\Lambda} \right) + i\frac{2\omega n_0}{c} \left( 1 \mp \frac{g(z)}{2n_0^2} \right) z \right] A_{\pm}^f(z) = 0, \quad (1b)$$

where  $\kappa = \omega a_c / 4c$  is the coupling coefficient of the grating. Noteworthy is here the decoupled form between orthogonal circular polarization states, stating that the modulation of the effective refractive index couples a circularly polarized component of the forward propagating field only to the backward travelling component of orthogonal polarization state, hence reversing the helicity of a circularly polarized optical field in reflection.

### Perturbation analysis of transmission properties

As they are stated, the coupled mode equations (1) provide a general description of wave propagation in spatially modulated media, for an arbitrary magneto-optical perturbation function  $g(z)$  and arbitrary apodization  $f(z)$ , within the validity region of slowly varying envelopes. Considering a sufficiently small chirp, with  $\xi L / \Lambda \ll 1$ , the phase function of the grating profile can be approximated as a polynomial

$$\frac{2\pi}{\xi} \ln \left( 1 + \frac{\xi z}{\Lambda} \right) \approx \frac{2\pi}{\Lambda} \left( 1 - \frac{\xi z}{2\Lambda} \right) z,$$

and by applying perturbation analysis of the direct scattering process described the coupled mode equations, the backscattered fields can expressed as the first-order integral solutions [3]

$$A_-^b(0) = -i\kappa A_+^f(0) \int_0^L f(z) \exp \left[ i\frac{2\omega n_0}{c} \left( 1 - \frac{g(z)}{2n_0^2} \right) z - i\frac{2\pi}{\Lambda} \left( 1 - \frac{\xi z}{2\Lambda} \right) z \right] dz, \quad (2a)$$

$$A_+^b(0) = -i\kappa A_-^f(0) \int_0^L f(z) \exp \left[ i\frac{2\omega n_0}{c} \left( 1 + \frac{g(z)}{2n_0^2} \right) z - i\frac{2\pi}{\Lambda} \left( 1 - \frac{\xi z}{2\Lambda} \right) z \right] dz, \quad (2b)$$

where terms of the order of  $O(\kappa^3)$  were omitted. From these integral expressions, the transmitted optical fields can similarly be constructed from the perturbation series as

$$A_+^f(L) = A_+^f(0) + i\kappa A_-^b(0) \int_0^L f(z) \exp \left[ -i\frac{2\omega n_0}{c} \left( 1 - \frac{g(z)}{2n_0^2} \right) z + i\frac{2\pi}{\Lambda} \left( 1 - \frac{\xi z}{2\Lambda} \right) z \right] dz, \quad (3a)$$

$$A_-^f(L) = A_-^f(0) + i\kappa A_+^b(0) \int_0^L f(z) \exp \left[ -i\frac{2\omega n_0}{c} \left( 1 + \frac{g(z)}{2n_0^2} \right) z + i\frac{2\pi}{\Lambda} \left( 1 - \frac{\xi z}{2\Lambda} \right) z \right] dz. \quad (3b)$$

The interpretation of the polarization state dependence of the obtained solutions is aided by the introduction of the Stokes parameters [4], which for the input optical field yield

$$\begin{aligned} S_0^{(\text{in})} &= |A_+^f(0)|^2 + |A_-^f(0)|^2, & S_1^{(\text{in})} &= 2\text{Re}[A_+^{f*}(0)A_-^f(0)], \\ S_3^{(\text{in})} &= |A_+^f(0)|^2 - |A_-^f(0)|^2, & S_2^{(\text{in})} &= 2\text{Im}[A_+^{f*}(0)A_-^f(0)], \end{aligned}$$

and similarly for the transmitted field

$$\begin{aligned} S_0^{(\text{tr})} &= |A_+^f(L)|^2 + |A_-^f(L)|^2, & S_1^{(\text{tr})} &= 2\text{Re}[A_+^{f*}(L)A_-^f(L)], \\ S_3^{(\text{tr})} &= |A_+^f(L)|^2 - |A_-^f(L)|^2, & S_2^{(\text{tr})} &= 2\text{Im}[A_+^{f*}(L)A_-^f(L)], \end{aligned}$$

in which  $S_0^{(\text{in})}$  and  $S_0^{(\text{tr})}$  are measures of the input and transmitted intensities, while  $S_3^{(\text{in})}$  and  $S_3^{(\text{tr})}$  determine the ellipticity of the corresponding polarization states.

### Discussion

For the numerical investigation of solutions to the coupled mode equations, the apodizing function  $f(z)$  was chosen as

$$f(z) = \begin{cases} [1 - \cos(\pi z/L_a)]/2, & \text{if } 0 \leq z < L_a, \\ 1, & \text{if } L_a \leq z \leq L - L_a, \\ [1 - \cos(\pi(z - L)/L_a)]/2, & \text{if } L - L_a < z \leq L, \end{cases}$$

where  $L_a$  is the effective apodization length. Intensity transmission spectra were calculated for a typical grating of length  $L = 20.0$  mm, index  $n_0 = 1.44$ , and peak modulation strength  $a = 1.0 \times 10^{-3}$ . Designing the grating to possess a flat window of reflection ranging from vacuum wavelength  $\lambda_a = 1530$  nm to  $\lambda_b = 1550$  nm, the initial grating period was chosen as  $\Lambda = \lambda_b/2n_0 = 538.2$  nm. In order for the grating to span over a 20 nm window of reflection, the chirp parameter was subsequently chosen as  $\xi = (\lambda_a - \lambda_b)/(2n_0L) = -347.2 \times 10^{-9}$ . In order to eliminate any Gibbs oscillations [5] in the spectrum, resulting from the grating boundaries, an apodization over  $L_a = 0.4$  mm was found sufficient.

The magneto-optically induced perturbation, which has the main impact of opening up for narrow transmission peak in the reflection band, was taken with a peak gyration coefficient of  $g_p = 0.7 \times 10^{-3}$ , perturbation width  $w_p = 0.3$  mm, and a centre position  $z_p = 10$  mm. The resulting calculated transmission spectra are shown in Fig. 2, for input optical fields being left (LCP, solid curve) and right (RCP, dashed curve) circularly polarized. As a consequence of the magneto-optically induced perturbation, in which the effective refractive index of the medium locally experiences a differential shift of its bias for orthogonal circular polarization states, the resonance peaks are slightly shifted to the left (for RCP) and right (for LCP) of the central resonance as determined by the local grating period of the chirped grating at the position of the perturbation. The spectral separation between the peaks for orthogonal circular polarization states as they appear in Fig. 2 is 0.6 nm, and the full width half maximum of each peak is 0.18 nm, hence providing a reasonable resolution for applications.

The high definition of the transmission peaks of LCP and RCP states as shown in Fig. 2 also suggests that in the region of the perturbation, the transmitted polarization state undergoes a radical change in its ellipticity, since the resonance of one polarization does not overlap with the resonance of the orthogonal state. That so actually also is the case is illustrated in Fig. 3, where the spectral dependence of the transmitted ellipticity  $S_3^{(\text{tr})}$  is shown for a linearly polarized input beam, assuming the same grating and magneto-optical perturbation parameters as in Fig. 2.

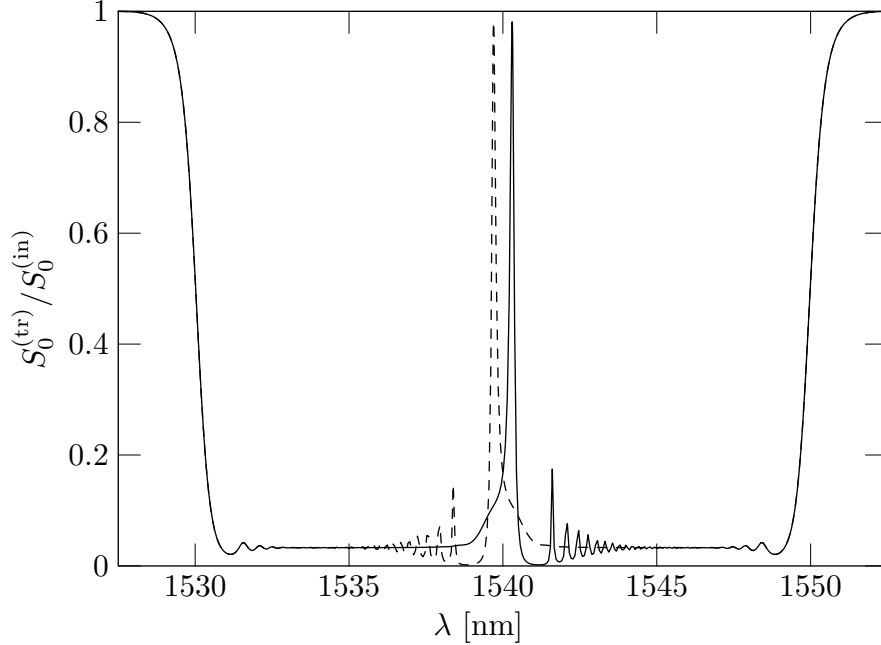


Figure 2: The intensity transmission as function of vacuum wavelength  $\lambda$ , for left and right circularly polarized input beam, drawn as solid and dashed curves, respectively. The shown spectra were calculated for a grating profile with length  $L = 20.0$  mm, bias index  $n_0 = 1.44$ , index modulation  $a = 1.0 \times 10^{-3}$ , peak gyration coefficient  $g_p = 0.7 \times 10^{-3}$ , perturbation width  $w_p = 0.3$  mm, geometrical initial period  $\Lambda = 538.2$  nm, chirp  $\xi = -347.2 \times 10^{-9}$ , and with an apodization over  $L_a = 0.4$  mm at each end of the grating.

At the ends of the spectrum, where the optical throughput is high, the feature introduced with a locally induced perturbation is clear; since the boundaries of the grating are left unperturbed, the polarization state selectivity there remains degenerate and a linearly polarized input will leave the transmitted polarization state as linear, except for in the region in which the perturbation acts. In addition, by changing the spatial position of the perturbation, hence changing the local resonance condition of the chirped grating, one may also exploit the tunability of the spectral positions of the transmission peaks. In this case, the primary control parameter is the positioning of the perturbation, while the strength of the magnetic field plays a secondary role, only providing the means to compensate for any fluctuations or deviations in grating quality along the axis of wave propagation.

**Conclusion**

In conclusion, we have in this paper reported on analysis of magneto-optical perturbations introduced over a macroscopic length scale, in weakly modulated chirped gratings. Coupled mode equations for the wave propagation in the perturbed medium were presented, and their solution using perturbation analysis was outlined. For the model grating used in the numerical evaluation, we predict a high polarization state selectivity induced in the region of the perturbation while still maintaining the window of operation intact.

The main impact of the present work is that it shows on the possibilities opened by

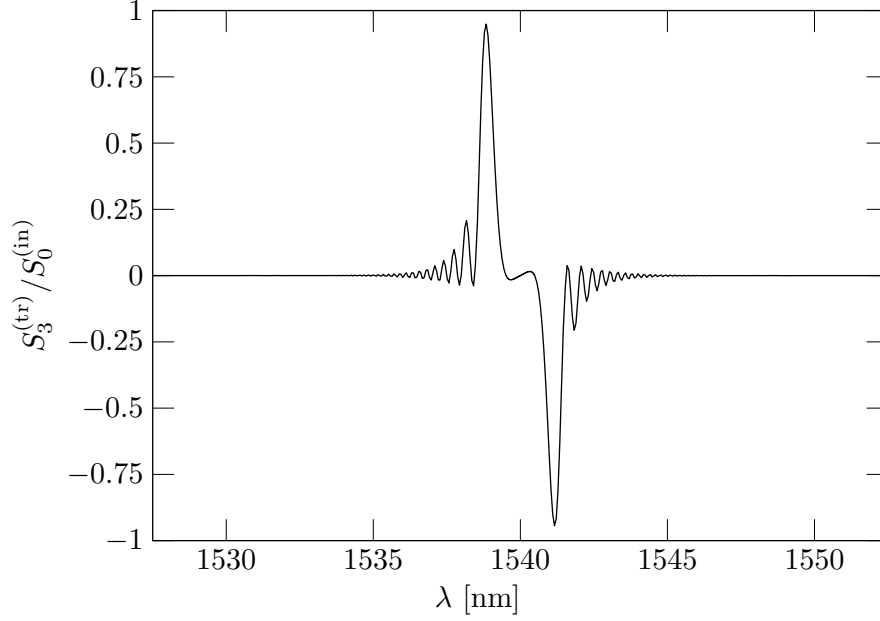


Figure 3: The transmitted ellipticity  $S_3^{(\text{tr})} = |A_+^f(L)|^2 - |A_-^f(L)|^2$  as function of vacuum wavelength  $\lambda$ , for a linearly polarized input beam ( $S_3^{(\text{in})} = 0$ ). The numerical parameters used are identical to those used for calculating the spectra in Fig. 2.

introducing magneto-optically induced perturbations of a macroscopic length scale, in gratings which need not to possess high index contrast, but which nevertheless can provide a considerably high spectral extinction ratio.

## References

1. L. D. Landau, E. M. Lifshitz, and L. P. Pitaevskiĭ, *Electrodynamics of Continuous Media*, 2nd ed. (Butterworth & Heinemann, Oxford, 1984).
2. Y. R. Shen, *The Principles of Nonlinear Optics* (Wiley, New York, 1984).
3. F. Jonsson and C. Flytzanis, *J. Nonlinear Opt. Phys. Mater.* **13**, 129–154 (2004).
4. M. Born and E. Wolf, *Principles of Optics*, 6th ed. (Cambridge University Press, Cambridge, 1980).
5. A. Othonos and K. Kalli, *Fiber Bragg Gratings* (Artech House, Boston, 1999).